J|A|C|S
ARTICLES
Published on Web 07/31/2002

# Singlet−Triplet Gap in Triplet Ground-State Biradicals Is Modulated by Substituent Effects

David A. Shultz,*,† Scot H. Bodnar,† Hyoyoung Lee,†,|| Jeff W. Kampf,‡ Christopher D. Incarvito,§ and Arnold L. Rheingold§

*Contribution from the Department of Chemistry, North Carolina State University, Raleigh, North Carolina 27695-8204, Department of Chemistry, University of Michigan, Ann Arbor, Michigan 48109-1055, and Department of Chemistry and Biochemistry, University of Delaware, Newark, Delaware 19716*

Received January 30, 2002

***Abstract:*** Three $S = 1$ bis(semiquinone) complexes have been prepared. To ensure ferromagnetic intramolecular exchange coupling, the two semiquinones are attached 1,3 to a 5-substituted phenylene ring. The biradical complexes differ in their meta-substituents: **1-NMe$_2$**, X = *N*,*N*-dimethylamino; **1-*t*-Bu**, X = *tert*-butyl; **1-NO$_2$**, X = nitro. All three structures have been determined by X-ray crystallography. Results of structural studies indicate that the biradical ligands of all three complexes have nearly identical conformations with average semiquinone ring torsions of 32° ± 2° relative to the 5-substituted phenylene ring. The exchange parameter, $J$ ($H = -2J\hat{S}_1\cdot\hat{S}_2$), ranges from +31.0 ± 0.6 cm$^{-1}$ for **1-NO$_2$** to +59.3 ± 1.2 cm$^{-1}$ for **1-*t*-Bu**, with $J = +34.9 \pm 0.7$ cm$^{-1}$ for **1-NMe$_2$**. Since the conformations are nearly identical, the differences in exchange coupling parameter $J$ are due to substituent effects. The experimental results are supported by Hückel theory arguments and previous computational work.

## Introduction

Preparation and electronic structure studies of high-spin organic molecules are main research topics in modern magnetochemistry. A major achievement in the field of organic biradicals was elucidating and measuring the relationship between $\pi$-connectivity and exchange coupling in triplet ground-state biradicals trimethylenemethane (TMM)[1−4] and *meta*-xylylene.[3,5−7] As a result of the theoretical understanding of this molecular structure−property relationship, several groups successfully designed and synthesized high-spin organic molecules based on structural elements of TMM and *meta*-xylylene (i.e., generalized *meta*-phenylene-type and generalized TMM-type biradicals, Figure 1).[8−13] Furthermore, it has been shown

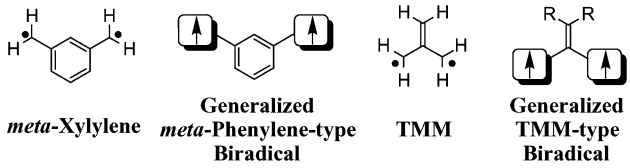


***Figure 1.*** *meta*-Xylylene and TMM and their generalized biradical analogues.

that bond torsions modulate the energy gap between triplet and singlet states ($\Delta E_{ST}$) by controlling delocalization between spin-containing groups and exchange coupling groups.[14−25]

Despite these landmark achievements, there has been no experimental demonstration of controlling $\Delta E_{ST}$ of a *triplet*

* To whom correspondence should be addressed. Voice: (919) 515-6972. E-mail: david_shultz@ncsu.edu. Fax: (919) 515-8920.
† North Carolina State University.
‡ University of Michigan.
§ University of Delaware.
|| Current address: Organic Materials Device Team, Telecommunication Basic Research, Electronics and Telecommunications Research Institute (ETRI), 161 Kajong-dong, Yusong-Gu, Taejon, 305-350, Korea.

(1) Dowd, P. *J. Am. Chem. Soc.* **1966**, *88*, 2587.
(2) Berson, J. A. *Acc. Chem. Res.* **1978**, *11*, 446.
(3) Borden, W. T.; Davidson, E. R. *J. Am. Chem. Soc.* **1977**, *99*, 4587.
(4) Wenthold, P. G.; Squires, R. R.; Lineberger, W. C. *J. Am. Chem. Soc.* **1996**, *118*, 475.
(5) Wright, B. B.; Platz, M. S. *J. Am. Chem. Soc.* **1983**, *105*, 628.
(6) Borden, W. T. *Diradicals*; Wiley: New York, 1982.
(7) Wenthold, P. G.; Kim, J. B.; Lineberger, W. C. *J. Am. Chem. Soc.* **1997**, *119*, 1354.
(8) Rajca, A. *Chem. Rev.* **1994**, *94*, 871.
(9) Dougherty, D. A. *Acc. Chem. Res.* **1991**, *24*, 88.
(10) Dougherty, D. A.; Jacobs, S. J.; Silverman, S. K.; Murray, M.; Shultz, D. A.; West, A. P., Jr.; Clites, J. A. *Mol. Cryst. Liq. Cryst.* **1993**, *232*, 289.
(11) Iwamura, H. *Pure Appl. Chem.* **1987**, *59*, 1595.
(12) Iwamura, H. *Adv. Phys. Org. Chem.* **1990**, *26*, 179.
(13) Iwamura, H. *Pure Appl. Chem.* **1993**, *65*, 57.
(14) Adam, W.; van Barneveld, C.; Bottle, S. E.; Engert, H.; Hanson, G. R.; Harrer, H. M.; Heim, C.; Nau, W. M.; Wang, D. *J. Am. Chem. Soc.* **1996**, *118*, 3974.
(15) Dvolaitzky, M.; Chiarelli, R.; Rassat, A. *Angew. Chem., Int. Ed. Engl.* **1992**, *31*, 180.
(16) Fang, S.; Lee, M.-S.; Hrovat, D. A.; Borden, W. T. *J. Am. Chem Soc.* **1995**, *117*, 6727.
(17) Fujita, J.; Tanaka, M.; Suemune, H.; Koga, N.; Matsuda, K.; Iwamura, H. *J. Am. Chem. Soc.* **1996**, *118*, 9347.
(18) Kanno, F.; Inoue, K.; Koga, N.; Iwamura, H. *J. Am. Chem. Soc.* **1993**, *115*, 847.
(19) Nakazono, S.; Karasawa, S.; Iwamura, H. *Angew. Chem., Int. Ed.* **1998**, *37*, 1550.
(20) Okada, K.; Matsumoto, K.; Oda, M.; Murai, H.; Akiyama, K.; Ikegami, Y. *Tetrahedron Lett.* **1995**, *36*, 6693.
(21) Okada, K.; Imakura, T.; Oda, M.; Murai, H.; Baumgarten, M. *J. Am. Chem. Soc.* **1996**, *118*, 3047.
(22) Shultz, D. A.; Boal, A. K.; Farmer, G. T. *J. Am. Chem. Soc.* **1997**, *119*, 3846.
(23) Shultz, D. A. *Conformational Exchange Modulation in Trimethylenemethane (TMM)-Type Biradicals*; Lahti, P., Ed.; Marcel Dekker: New York, 1999.
(24) Shultz, D. A.; Boal, A. K.; Lee, H.; Farmer, G. T. *J. Org. Chem.* **1999**, *64*, 4386.
(25) Silverman, S. K.; Dougherty, D. A. *J. Phys. Chem.* **1993**, *97*, 13273.


**10.1021/ja020154+ CCC: $22.00** 

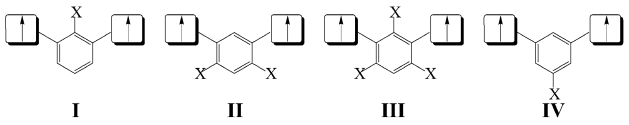


***Figure 2.*** Substitution patterns for *meta*-phenylene-type biradicals.

*ground-state* biradical, other than by bond torsions.[23,25,26] On the other hand, Berson reported that electron-withdrawing substituents modulate the singlet−triplet gaps of *singlet ground-state* tetramethylene*ethane*-type biradicals.[27−29] In addition, Borden,[30] Dougherty,[31] Hadad,[32] and Yamaguchi[33] reported substituent effects on exchange coupling in computational studies. Thus, pure electronic modulation of coupling within an isostructural series of *triplet ground-state*, conjugated biradicals has not been achieved experimentally. Herein, we demonstrate the existence of a substituent effect on exchange coupling in *meta*-phenylene-type biradicals with substituted coupler fragments.

Substituted exchange couplers could alter $\Delta E_{ST}$ of a triplet ground-state biradical in several ways, including selective change in the lowest singlet-state energy (case A), selective change in the triplet-state energy (case B), or energy changes in both states (case C).[34] Figure 2 shows four different, $C_2$-symmetric *meta*-phenylene-type biradicals. In derivatives I−III, mesomeric substituents, X, may be in conjugation with the spin-containing fragments and, in the absence of additional functionality, will cause torsion of the spin-containing fragments with respect to the coupler fragment. Derivative IV has its single substituent meta to the spin-containing groups, so no conjugation between X and the spin-containing groups is possible.

Derivatives I−IV could affect $\Delta E_{ST}$ by any of the three mechanistic cases mentioned above; furthermore, ortho-/para-substituents (derivatives I−III) might affect $\Delta E_{ST}$ differently than meta-substituents (derivative IV). Because molecular design issues (e.g., degree of planarity) and syntheses are more straightforward for derivative IV than for derivatives I−III, we focus here on *meta*-phenylene-substituted, bis(semiquinone) biradicals **1-NMe$_2$**, **1-*t*-Bu**, and **1-NO$_2$** (see Chart 1) to demonstrate experimentally that substituents affect exchange coupling.

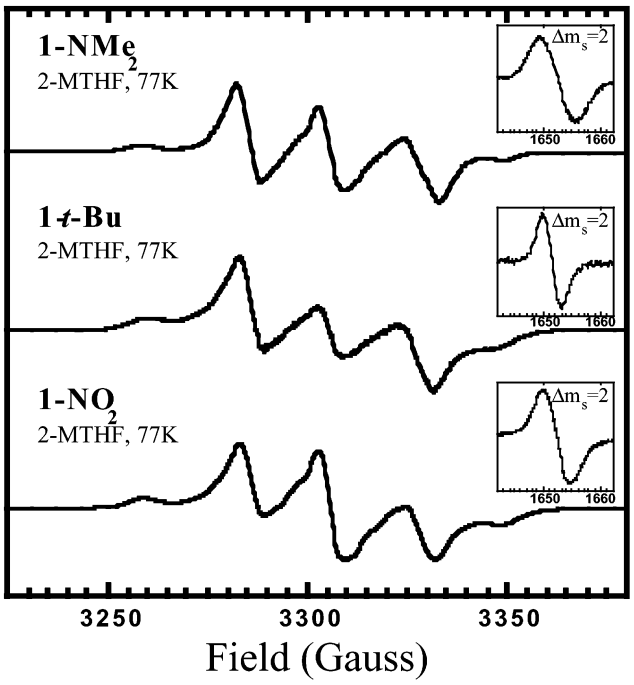


***Figure 3.*** EPR spectra of **1-NMe$_2$**, **1-*t*-Bu**, and **1-NO$_2$** recorded at 77 K in a 2-MTHF glass. Zero-field splitting parameters were estimated by simulations: **1-NMe$_2$**, $|D/hc| = 0.004\ 28\ cm^{-1}$, $|E/hc| = 0.000\ 187\ cm^{-1}$; **1-*t*-Bu**, $|D/hc| = 0.004\ 14\ cm^{-1}$, $|E/hc| = 0.000\ 140\ cm^{-1}$; **1-NO$_2$**, $|D/hc| = 0.004\ 23\ cm^{-1}$, $|E/hc| = 0.000\ 047\ cm^{-1}$. Insets: $\Delta m_s = 2$ transitions.

## Results and Discussion

**Synthesis.** All three bis(semiquinone) complexes contain the hydrotris(3-methyl-5-cumenylpyrazolyl)borate ($Tp^{Cum,Me}$) ancillary ligand.[35−37] This large, encapsulating ligand limits the number of conformational degrees of freedom for the bis(semiquinone)s and isolates the bis(semiquinone)s in the solid state, attenuating the effect of intermolecular forces on both molecular conformation and magnetic properties. Complexes **1-NMe$_2$**, **1-*t*-Bu**, and **1-NO$_2$** were prepared by the reaction of $Tp^{Cum,Me}$ZnOH with a bis(catechol) as reported for another bis(semiquinone) complex,[38,39] following the general procedure of Pierpont as indicated in Scheme 1.[36,37]

Bis(catechol)s **6** and **8** were prepared as shown in Scheme 1, following our previously reported procedure for **7** via **4**.[40] Dibromides **3**[41] and **5**[42] were prepared according to literature methods.

**Electron Paramagnetic Resonance Spectroscopy.** Frozen-solution electron paramagnetic resonance (EPR) spectroscopy has been used extensively to study biradicals.[8,43] In the present case, we wished to determine if the substituents caused a measurable change in the triplet zero-field splitting parameters characteristic of different spin density distributions. Figure 3

(26) Nocera and Jackson have shown substituent effects on magnetic ordering of vanadyl arylphosphonates by altering phenyl substituents on the phosphonate ligands; see: Bideau, J. L.; Papoutsakis, D.; Jackson, J. E.; Nocera, D. G. *J. Am. Chem. Soc.* **1997**, *119*, 1313. However, in this case, the different phosphonates had different V−O bond lengths that attenuate the *direct* exchange interaction.
(27) Bush, L.; Heath, R.; Feng, X.; Wang, P.; Maksimovic, L.; Song, A.; Chung, W.; Berinstain, A.; Scaiano, J.; Berson, J. *J. Am. Chem. Soc.* **1997**, *119*, 1406.
(28) Berson, J. A. *Acc. Chem. Res.* **1997**, *30*, 238.
(29) Berson, J. A. *Structural Determinants of the Chemical and Magnetic Properties of Non-Kekulé Molecules*; Lahti, P., Ed.; Marcel Dekker: New York, 1999; pp 7−26.
(30) Adam, W.; Borden, W. T.; Burda, C.; Foster, H.; Heidenfelder, T.; Heubes, M.; Hrovat, D.; Kita, F.; Lewis, S.; Scheutzow, D.; Wirz, J. *J. Am. Chem. Soc.* **1998**, *120*, 593.
(31) West, A. P., Jr.; Silverman, S. K.; Dougherty, D. A. *J. Am. Chem. Soc.* **1996**, *118*, 1452.
(32) Geise, C. M.; Hadad, C. M. *J. Org. Chem.* **2000**, *65*, 8348.
(33) Mitani, M.; Yamaki, D.; Takano, Y.; Kitagawa, Y.; Yoshioka, Y.; Yamaguchi, K. *J. Chem. Phys.* **2000**, *113*, 10486.
(34) The two-orbital, two-electron model predicts four electronic states. For our purposes, we are considering only the lowest lying singlet and triplet states. For a detailed discussion of biradical electronic structure, see refs 6, 8, 9, and the following: Salem, L.; Rowland, C. *Angew. Chem., Int. Ed. Engl.* **1972**, *11*, 92. Michl, J.; Bonacic-Koutecky, V. *Electronic Aspects of Organic Photochemistry*; Wiley-Interscience: New York, 1990.
(35) Ruf, M.; Vahrenkamp, H. *Inorg. Chem.* **1996**, *35*, 6571.
(36) Ruf, M.; Noll, B. C.; Groner, M. D.; Yee, G. T.; Pierpont, C. G. *Inorg. Chem.* **1997**, *36*, 4860.
(37) Ruf, M.; Lawrence, A. M.; Noll, B. C.; Pierpont, C. G. *Inorg. Chem.* **1998**, *37*, 1992.
(38) Shultz, D. A.; Bodnar, S. H. *Inorg. Chem.* **1999**, *38*, 591.
(39) Shultz, D. A.; Bodnar, S. H.; Kumar, R. K.; Kampf, J. W. *J. Am. Chem. Soc.* **1999**, *121*, 10664.
(40) Shultz, D. A.; Boal, A. K.; Driscoll, D. J.; Kitchin, J. R.; Tew, G. N. *J. Org. Chem.* **1995**, *60*, 3578.
(41) Vorländer, D.; Siebert, E. *Chem. Ber.* **1919**, *52*, 283.
(42) Bhandari, G.; Rheingold, A. L.; Theopold, K. H. *Chem.−Eur. J.* **1995**, *1*, 199.
(43) Dougherty, D. A. In *Matrix Isolation EPR Spectroscopy of Biradicals*; Platz, M. S., Ed.; Plenum Press, New York, 1990; pp 117−142.

***Chart 1***

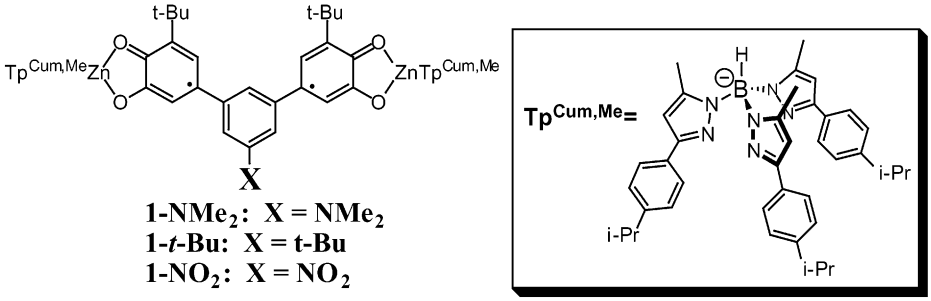


**1-NMe$_2$: X = NMe$_2$**
**1-*t*-Bu: X = t-Bu**
**1-NO$_2$: X = NO$_2$**

***Scheme 1***

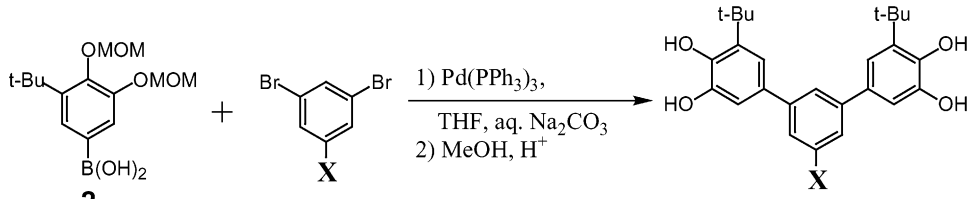


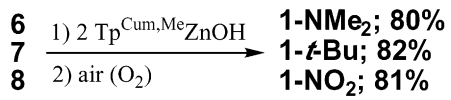


***Table 1.*** Crystal Data and Structure Refinement for **1-NMe$_2$**, **1-*t*-Bu**, and **1-NO$_2$**

| empirical formula | $C_{109}H_{129}B_2Cl_6N_{13}O_4Zn_2$ (**1-NMe$_2$**·3$CH_2Cl_2$) | $C_{111}H_{132}B_2N_{12}O_4Zn_2Cl_6$ (**1-*t*-Bu**·3$CH_2Cl_2$) | $C_{106}H_{121}B_2N_{13}O_6Zn_2Cl_4$ (**1-NO$_2$**·2$CH_2Cl_2$) |
|---|---|---|---|
| *a*/Å | 12.432(3) | 12.688(5) | 12.460(2) |
| *b*/Å | 13.006(3) | 12.987(5) | 13.048(2) |
| *c*/Å | 33.338(7) | 33.514(12) | 33.278(6) |
| α/deg | 97.952(10) | 99.258(6) | 97.901(3) |
| *β*/deg | 94.198(11) | 92.264(7) | 95.124(3) |
| *γ*/deg | 97.345(14) | 97.887(6) | 97.495(3) |
| *V*/Å$^3$ | 5271.8(19) | 5388(3) | 5281.2(17) |
| Z | 2 | 2 | 2 |
| formula weight | 1878.03 | 2050.31 | 1750.45 |
| crystal system, space group | triclinic, $P\bar{1}$ (green plate) | triclinic, $P\bar{1}$ (green plate) | triclinic, $P\bar{1}$ (green plate) |
| *T*/K | 173(2) | 158(2) | 158(2) |
| *λ*/Å | 0.7071 | 0.7071 | 0.7071 |
| $\delta_{calc}$/g cm$^{-3}$ | 1.292 | 1.266 | 1.237 |
| *μ*/cm$^{-1}$ | 6.65 | 6.50 | 6.13 |
| *R*(*F*) | 0.1352 | 0.0973 | 0.1231 |
| $R_w(F^2)$ | 0.2772 | 0.2643 | 0.3197 |

shows the X-band EPR spectra of **1-NMe$_2$**, **1-*t*-Bu**, and **1-NO$_2$** recorded at 77 K in 2-MTHF. All of the spectra are characteristic of triplet states and exhibit $\Delta m_s = 2$ signals near half-field. Simulations[44] were achieved using $|D/hc| \approx 0.0042$ cm$^{-1}$ and $|E/hc| \approx 0.0001$ cm$^{-1}$ for all three compounds (see Supporting Information). Curie plots (not shown) of the doubly integrated $\Delta m_s = 2$ signals are linear, suggesting $J \geq 0$, that is, ferromagnetic coupling. Since the zero-field splitting parameters are nearly identical for all three compounds, we conclude that either the spin density distributions are nearly identical in the three biradicals or any differences in spin densities are too small to be measured by frozen-solution EPR spectroscopy.

**Molecular Structures.** X-ray-quality crystals of complexes **1-NMe$_2$**, **1-*t*-Bu**, and **1-NO$_2$** were analyzed by X-ray crystallographic techniques. Crystallographic data are given in Table 1, and ORTEPs are shown in Figure 4. Bond lengths are given in Table 2, while important torsion angles are listed in Table 3.

All dioxolene ring C−O and C−C bond lengths are in accord with the semiquinone oxidation state.[45,46] Since we are focusing on substituent effects, the most important structural parameters other than the semiquinone bond lengths are the semiquinone ring torsion angles relative to the central *meta*-phenylene couplers. It is imperative that these torsion angles be nearly identical if we are to attribute differences in exchange coupling predominantly to substituent effects and not to a combination of substituent effects and bond torsions.

As can be seen in Table 3, the conformations of **1-NMe$_2$**, **1-*t*-Bu**, and **1-NO$_2$** are nearly identical with an average

(44) Bruker *WINEPR SimFonia*, 1.25, shareware version; Brüker Analytische Messtechnik GmbH: Rheinstetten, Germany, 1996.

(45) Pierpont, C. G.; Buchanan, R. M. *Coord. Chem. Rev.* **1981**, *38*, 45.
(46) Pierpont, C. G.; Lange, C. W. *Prog. Inorg. Chem.* **1994**, *41*, 331.

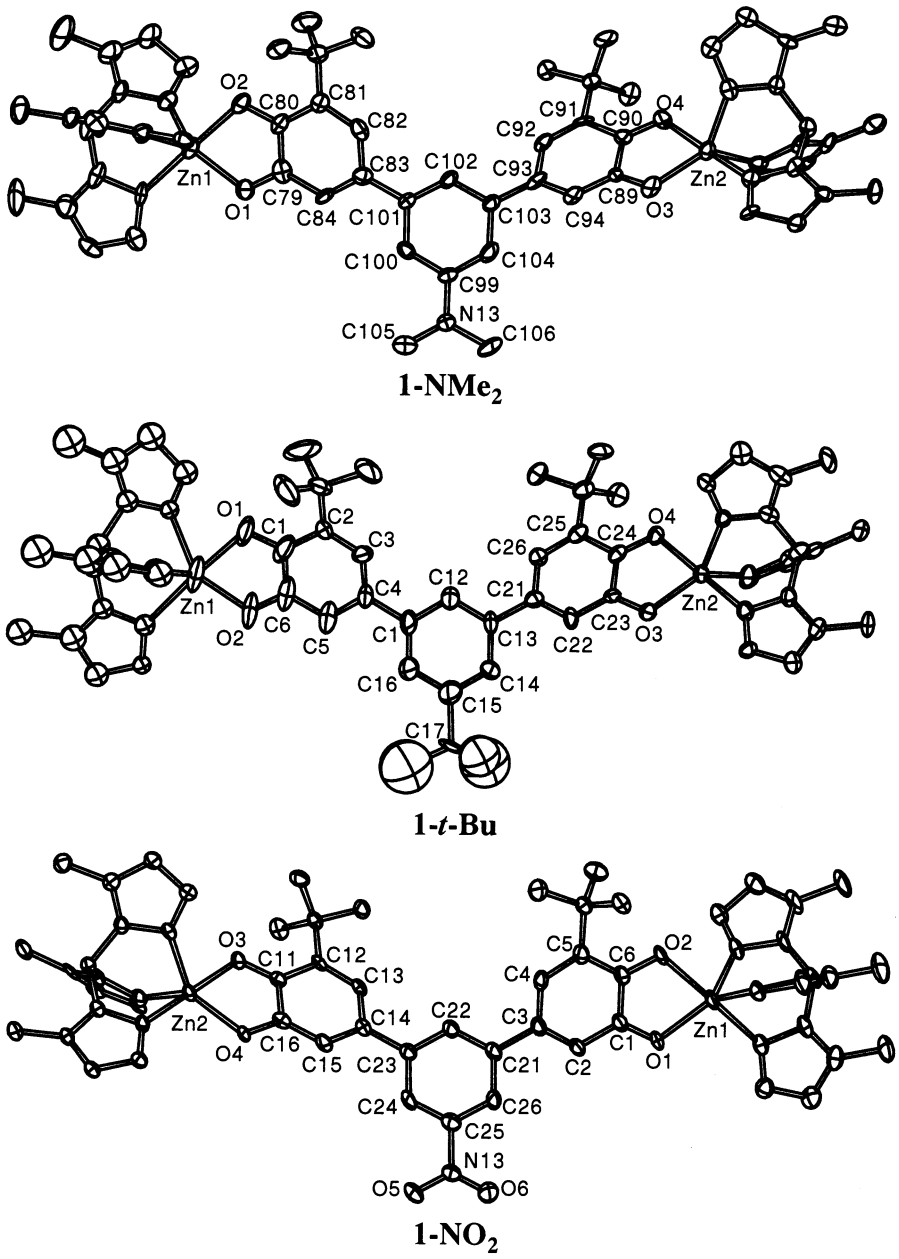


***Figure 4.*** ORTEPs of **1-NMe$_2$**, **1-*t*-Bu**, and **1-NO$_2$**. Hydrogens and cumenyl groups have been omitted for clarity.

semiquinone ring torsion of 32.4° ± 2.0° relative to the central substituted phenyl ring. We consider this conformational variation negligible, that is, not of a magnitude that could have a measurable effect on exchange coupling.

**Magnetic Susceptibility Studies.** The magnetic susceptibilities of **1-NMe$_2$**, **1-*t*-Bu**, and **1-NO$_2$** were measured from 2 to 300 K using a SQUID magnetometer with an applied magnetic field of 1 T and are plotted as $\chi T$ products in Figure 5. The room-temperature $\chi T$ values for all three complexes are greater than the value for two uncorrelated spins ($\chi T = 0.75$ emu K/mol), consistent with ferromagnetic intramolecular exchange interactions. In addition, the $\chi T$ value for each complex *increases* as the temperature is lowered. Thus, the shapes of the $\chi T$ plots are consistent with $J > 0$ for all three complexes and with $J$(**1-NO$_2$**) < $J$(**1-NMe$_2$**) < $J$(**1-*t*-Bu**).

Modeling the temperature-dependent $\chi T$ products of $S = 1$ molecules can be achieved by fitting to a field-independent van Vleck expression (using $\mathrm{H} = -2J\hat{S}_1\cdot\hat{S}_2$), eq 1.[47,48]

$$\chi T = \frac{2Ng^2\beta^2}{k[3 + \mathrm{e}^{-2J/kT}]} \qquad (1)$$

where $g$ is the isotropic Landé constant ($g = 2.0023$), $\beta$ is the Bohr magneton, $T$ is the temperature in Kelvin, $k$ is Boltzmann's constant, $J$ is the intramolecular semiquinone−semiquinone exchange coupling parameter ($2J = \Delta E_{ST}$), and $\hat{S}_1$ and $\hat{S}_2$ are the spin operators for the semiquinones. The decrease in the $\chi T$ data at low temperatures was accounted for with a Weiss correction, using the expression $\chi_{\mathrm{eff}} = \chi/(1 - \vartheta\chi)$, where $\vartheta = 2zJ'/(Ng^2\beta^2)$.[49] The origin of $J'$ may be zero-field splitting, intermolecular interaction, saturation effects, or some combina-

(47) Kahn, O. *Molecular Magnetism*; VCH: New York, 1993.
(48) Bleaney, B.; Bowers, K. D. *Proc. R. Soc. London* **1952**, *A214*, 451.
(49) O'Connor, C. J. *Prog. Inorg. Chem.* **1982**, *29*, 203.

***Table 2.*** Important Bond Lengths for **1-NMe$_2$**, **1-*t*-Bu**, and **1-NO$_2$**

| biradical | bond | length (Å) | bond | length (Å) |
|---|---|---|---|---|
| **1-NMe$_2$** | C79−O1 | 1.307(10) | C89−O3 | 1.272(12) |
| [semiquinone rings] | C79−C80 | 1.466(12) | C89−C90 | 1.463(15) |
| | C80−O2 | 1.248(11) | C90−O4 | 1.273(11) |
| | C80−C81 | 1.465(13) | C90−C91 | 1.428(14) |
| | C81−C82 | 1.326(13) | C91−C92 | 1.382(14) |
| | C82−C83 | 1.424(13) | C92−C93 | 1.437(15) |
| | C83−C84 | 1.396(13) | C93−C94 | 1.342(14) |
| | C84−C79 | 1.363(13) | C94−C89 | 1.421(13) |
| [SQ-phenylene] | C83−C101 | 1.458(14) | C93−C103 | 1.4741(3) |
| [*m*-phenylene ring] | C101−C102 | 1.407(13) | C103−C102 | 1.359(13) |
| | C101−C100 | 1.432(14) | C103−C104 | 1.437(14) |
| | C100−C99 | 1.364(14) | C104−C99 | 1.403(13) |
| [NMe$_2$ group] | C99−N13 | 1.386(13) | N13−C105 | 1.470(13) |
| | N13−C106 | 1.415(13) | | |
| [metal bond lengths] | Zn1−O1 | 1.960(7) | Zn2−O3 | 1.973(7) |
| | Zn1−O2 | 2.116(6) | Zn2−O4 | 2.110(7) |
| | Zn1−N1 | 2.034(8) | Zn2−N7 | 2.052(8) |
| | Zn1−N3 | 2.208(8) | Zn2−N9 | 2.147(9) |
| | Zn1−N5 | 2.024(9) | Zn2−N11 | 2.027(8) |
| **1-*t*-Bu** | C6−O2 | 1.312(6) | C23−O3 | 1.308(8) |
| [semiquinone rings] | C6−C1 | 1.475(7) | C23−C24 | 1.479(11) |
| | C1−O1 | 1.263(6) | C24−O4 | 1.268(7) |
| | C1−C2 | 1.456(6) | C25−C26 | 1.449(11) |
| | C2−C3 | 1.373(7) | C26−C21 | 1.379(8) |
| | C3−C4 | 1.428(7) | C21−C22 | 1.424(9) |
| | C4−C5 | 1.391(7) | C22−C6 | 1.382(9) |
| | C5−C6 | 1.382(7) | C6−C23 | 1.392(8) |
| [SQ-phenylene] | C4−C11 | 1.479(7) | C21−C23 | 1.486(7) |
| [*m*-phenylene ring] | C11−C12 | 1.390(7) | C13−C12 | 1.394(8) |
| | C11−C16 | 1.407(8) | C13−C14 | 1.405(9) |
| | C16−C15 | 1.394(10) | C14−C15 | 1.386(10) |
| | C15−C17 | 1.615(13) | | |
| [metal bond lengths] | Zn1−O2 | 1.978(3) | Zn2−O3 | 2.021(5) |
| | Zn1−O1 | 2.120(3) | Zn2−O4 | 2.023(7) |
| | Zn1−N1 | 2.197(4) | Zn2−N7 | 2.002(5) |
| | Zn1−N3 | 2.049(4) | Zn2−N9 | 2.486(16) |
| | Zn1−N5 | 2.034(4) | Zn2−N11 | 1.976(10) |
| **1-NO$_2$** | C16−O4 | 1.300(8) | C1−O1 | 1.286(9) |
| [semiquinone rings] | C16−C11 | 1.476(9) | C1−C6 | 1.456(10) |
| | C11−O3 | 1.271(8) | C6−O2 | 1.265(8) |
| | C11−C12 | 1.449(9) | C6−C5 | 1.455(10) |
| | C12−O13 | 1.367(9) | C5−C4 | 1.381(10) |
| | C13−C14 | 1.428(10) | C4−C3 | 1.433(11) |
| | C14−C15 | 1.388(9) | C3−C2 | 1.376(11) |
| | C15−C16 | 1.383(10) | C2−C1 | 1.425(10) |
| [SQ-phenylene] | C14−C23 | 1.478(10) | C3−C21 | 1.490(10) |
| [*m*-phenylene ring] | C23−C22 | 1.404(10) | C21−C22 | 1.400(10) |
| | C23−C24 | 1.411(10) | C21−C26 | 1.414(10) |
| | C24−C25 | 1.381(11) | C26−C25 | 1.385(11) |
| [NO$_2$ group] | C25−N13 | 1.484(10) | N13−O5 | 1.223(10) |
| | N13−O6 | 1.214(10) | | |
| [metal bond lengths] | Zn2−O4 | 1.986(5) | Zn1−O1 | 1.976(5) |
| | Zn2−O3 | 2.123(4) | Zn1−O2 | 2.124(5) |
| | Zn2−N7 | 2.050(6) | Zn1−N1 | 2.160(6) |
| | Zn2−N9 | 2.049(6) | Zn1−N3 | 2.040(6) |
| | Zn2−N11 | 2.192(5) | Zn1−N5 | 2.049(7) |

***Table 3.*** Semiquinone Ring Torsion Angles[a] for **1-NMe$_2$**, **1-*t*-Bu**, and **1-NO$_2$**

| biradical | semiquinone ring torsion angles (deg) | average semiquinone ring torsion angles (deg) |
|---|---|---|
| **1-NMe$_2$** | 36.0 ± 0.5, 31.0 ± 0.5 | 33.5 ± 0.5 |
| **1-*t*-Bu** | 30.2 ± 0.3, 30.8 ± 0.4 | 30.5 ± 0.4 |
| **1-NO$_2$** | 33.3 ± 0.3, 33.5 ± 0.4 | 33.4 ± 0.4 |

[a] Torsion angle is defined as the angle between the plane of a semiquinone ring and the plane of the central phenylene ring.

tion of these.[50] The other terms have their usual meanings.[49] The curve fit results are presented in Table 4.

Recently, we reported the magnetic properties of the bis(semiquinone) ligand portion of **1-*t*-Bu** complexed to two Cr$^{III}$, Ni$^{II}$, and Cu$^{II}$ ions.[51] The results of magnetic susceptibility studies indicated that the intraligand coupling ranged from +3 to +16 cm$^{-1}$, less than the *J*-value reported here (+59 cm$^{-1}$). However, the previously reported complexes were not structurally characterized, they were salts with counterions, and the ancillary ligands differed from those in the present cases. These differences, and the lack of structural information, render uncertain the bis(semiquinone) ligand conformation. Since there is ample precedent for bond torsions attenuating *J*,[23] we suggest that the previously reported Cr$^{III}$, Ni$^{II}$, and Cu$^{II}$ metal complexes have greater semiquinone ring torsion angles than the complexes reported here.

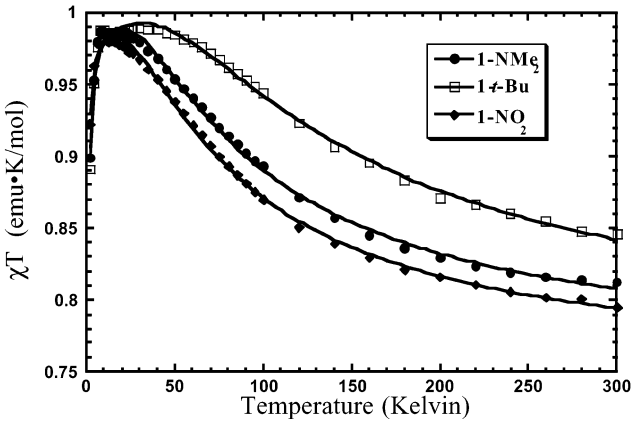


***Figure 5.*** Temperature dependence of $\chi T$ for biradicals **1-NMe$_2$**, **1-*t*-Bu**, and **1-NO$_2$**.

***Table 4.*** Variable-Temperature Susceptibility Fit Parameters for **1-NMe$_2$**, **1-*t*-Bu**, and **1-NO$_2$**[a]

| biradical | $J$ (cm$^{-1}$)[b] | $zJ'$ (cm$^{-1}$)[c] |
|---|---|---|
| **1-NMe$_2$** | +34.9 ± 0.7 | −0.11 ± 0.01 |
| **1-*t*-Bu** | +59.3 ± 1.2 | −0.11 ± 0.01 |
| **1-NO$_2$** | +31.0 ± 0.6 | −0.07 ± 0.01 |

[a] The fits used $g = 2.002$. [b] $J > 0$ for the triplet ground-state. [c] Intermolecular interaction.

The intermolecular interaction terms, $zJ'$, given in Table 4 are over 2 orders of magnitude smaller than the exchange parameters, *J*, consistent with the sterically bulky Tp$^{Cum,Me}$ ligand magnetically insulating the individual molecules in the solid state. Zero-field splitting can contribute to $zJ'$, but $|D/hc|$ is ca. 0.004 cm$^{-1}$, 4 orders of magnitude less than *J*.

**The Exchange Coupling is Substituent Modulated.** To date, there is no reported experimental study that correlates bond torsions with exchange coupling parameters within an isostructural series of biradicals. There are, however, several reports of individual examples of large torsions that change ferromagnetically coupled systems into antiferromagnetically or weakly coupled systems.[23] Therefore, we cannot be certain of the effects of very small bond torsion differences, such as those reported here, on exchange coupling. However, it seems reasonable that *J* should vary as $\cos(\phi)^2$, where $\phi$ is the torsion angle between the spin-containing units (semiquinones in the present case) and the coupling unit (*meta*-phenylene in the present case). The smallest *average* semiquinone ring torsion angle reported here is 30° ($\cos(\phi)^2 = 0.75$), and the largest is 34° ($\cos(\phi)^2 = 0.69$).

(50) Caneschi, A.; Dei, A.; Mussari, C. P.; Shultz, D. A.; Sorace, L.; Vostrikova, K. E. *Inorg. Chem.* **2002**, *41*, 1086.
(51) Caneschi, A.; Dei, A.; Lee, H.; Shultz, D. A.; Sorace, L. *Inorg. Chem.* **2001**, *40*, 408.

***Scheme 2***

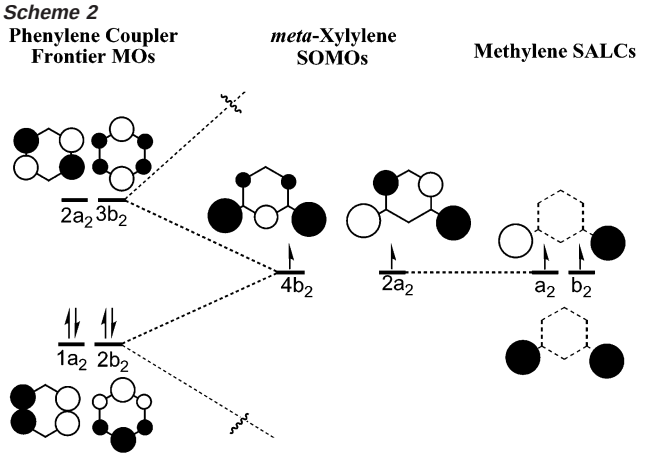


***Scheme 3***

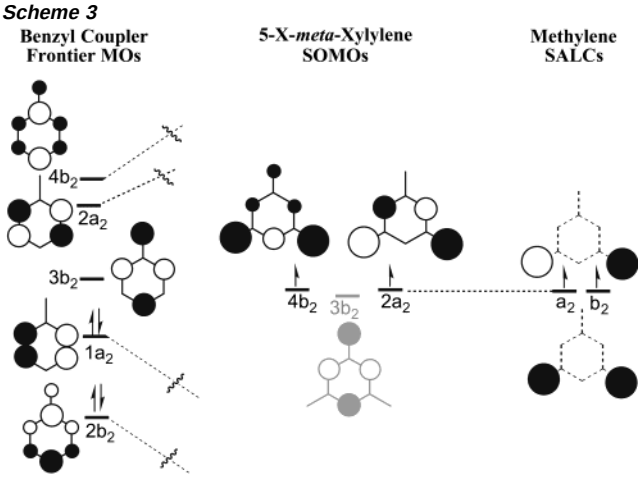


We feel confident that the small difference in the $\cos(\phi)^2$ values for these average torsion angles alone cannot be responsible for the observed 2-fold difference in $J$ and that the singlet−triplet gaps are a function of the phenylene ring substituents, X. At this point, it is also appropriate to note that semiquinones are radical *anions*, and the substituent effects described here for the *meta*-phenylene coupler could be limited to bis(semiquinone)s or other biradicals built from radical ions. Nevertheless, substituent effects modulate exchange coupling and can be used to *electronically* alter the exchange coupling ability of a functional group in high-spin ground-state molecules.

**On the Mechanism of Substituent Modulation of Exchange Coupling.** Accurate calculation of the exchange coupling parameter from a molecular orbital (MO) perspective must include configuration interaction.[47] However, MO theory alone *is* useful for determining the magnitude of the ferromagnetic contribution (the exchange integral) to the exchange parameter.[3,52,53]

In this way, simple perturbation theory in conjunction with Hückel MO theory provides a possible mechanism for $J$-modulation by substituents. Consider the MO interaction diagram in Scheme 2. For construction of the SOMOs of *meta*-xylylene using group theory as a guideline, the $a_2$ and $b_2$ symmetry-adapted linear combinations (SALCs) for the $CH_2$ radical fragments (Scheme 2, right) interact with the $1a_2/2a_2$ and $2b_2/3b_2$ frontier MOs of benzene (formally $e_{1g}$ and $e_{2u}$ for $D_{6h}$ symmetry), respectively. Because of the pairing theorem,[54] each set of interactions are equal in magnitude, resulting in two accidentally degenerate SOMOs. Indeed, the results of these orbital mixings are the well-known symmetrized SOMOs of the triplet ground-state *meta*-xylylene biradical.

Now consider attaching a mesomeric substituent to the benzene ring coupler: the $2b_2/3b_2$ MOs will mix with the substituent AO, but the $1a_2/2a_2$ will not interact with the substituent AO (Scheme 3). The results are the recognizable benzyl frontier MOs, shown to the left in Scheme 3. To continue, if one interacts the $a_2$ and $b_2$ SALCs for the $CH_2$ radical fragments with benzyl frontier MOs, the interaction of the $a_2$ $CH_2$-SALC will be identical to that in *meta*-xylylene, but the interaction of the $b_2$ $CH_2$-SALC will be attenuated because of the larger energy gap between the $b_2$ $CH_2$-SALC and the benzyl $2b_2$ and $4b_2$ SALCs. In addition, the substituent coefficient in the resultant $4b_2$ MO is nonzero. The weaker interaction and delocalization over the substituent conspire to attenuate the overlap density of the SOMOs and therefore decrease the exchange integral.[3,8,9] Put another way, the SOMOs are more disjoint than those of *meta*-xylylene. This explanation is independent of whether the $3b_2$ 5-X-*meta*-xylylene orbital is filled or unfilled; both electron pair donors *and* electron pair withdrawers are predicted to attenuate the exchange integral. Indeed, Borden and Squires have calculated the singlet−triplet gap in 1,3,5-trimethylene benzene monoanion (5-X-*meta*-xylylene, X = $CH_2^-$) to be ca. 5.0 kcal/mol, approximately 50% of the value for *meta*-xylylene.[55] They attributed the attenuated exchange coupling, in part, to more disjoint SOMOs.

## Conclusions

We demonstrated $J$-modulation through substituents in triplet ground-state biradicals. Our results show that a strong withdrawing group (X = $NO_2$) attenuates the singlet−triplet gap more than a strong donating group (X = $NMe_2$) relative to a weakly donating group (X = *tert*-butyl). Simple Hückel MO arguments, reinforced with previous computational work, suggest that strong electron donors *and* withdrawers reduce the ferromagnetic portion of the exchange parameter by attenuating the exchange integral (Case B), in accord with our experimental trend in $J$.

## Experimental Section

Unless noted otherwise, reactions were carried out in oven-dried glassware under a nitrogen atmosphere. Tetrahydrofuran (THF) and toluene were distilled under argon from sodium benzophenone ketyl, and methylene chloride and methanol were distilled from $CaH_2$ under argon. Other chemicals were purchased from Aldrich Chemical Co. Column and radial chromatography were carried out using silica gel (230−400 mesh for column). X-Band EPR spectroscopy was performed as described previously.[56] NMR spectra were recorded at 300 MHz for $^1$H NMR and 75 MHz for $^{13}$C NMR in $CD_2Cl_2$ solution if not otherwise specified. Elemental analyses were performed by Atlantic Microlab, Inc., Norcross, GA. Mass spectrometry was carried out at the NC State University Mass Spectrometry Facility.

(52) Borden, W. T.; Davidson, E. R. *Acc. Chem. Res.* **1981**, *14*, 69.
(53) Borden, W. T.; Iwamura, H.; Berson, J. A. *Acc. Chem. Res.* **1994**, *24*, 109.
(54) Salem, L. *Molecular Orbital Theory of Conjugated Systems*; W. A. Benjamin, Inc.: New York, 1966.
(55) Kemnitz, C. R.; Squires, R. R.; Borden, W. T. *J. Am. Chem. Soc.* **1997**, *119*, 6564.
(56) Shultz, D. A.; Farmer, G. T. *J. Org. Chem.* **1998**, *63*, 6254.

Compounds **2**, **4**, **7**,[40] **3**,[41] and **5**[42] were prepared as described previously. Metal complexes were prepared from the corresponding bis(catechol)s and $Tp^{Cum,Me}ZnOH$[35,36,57] as described previously.[39,58−60]

**5,5″-Di-*tert*-butyl-3,4,3″,4″-tetrakis-methoxymethoxy-5′-*N*,*N*-dimethylamino-[1,1′,3′,1″]terphenyl.** A 100 mL flask containing 1,3-dibromo-5-*N*,*N*-dimethylaminobenzene, **3**[41] (85 mg, 0.31 mmol), boronic acid **2**[40] (0.19 g, 0.64 mmol), $Pd(PPh_3)_4$ (40 mg, 0.03 mmol), EtOH (1.3 mL), and 40 mL of distilled THF was pump/purged three times under nitrogen. Aqueous $Na_2CO_3$ (2 mL, 2 M) was then added, and the reaction mixture was pumped/purged three more times and heated to reflux for 18 h. Once cool, the solvent was removed under reduced pressure, ether was added, and the reaction mixture was filtered to remove inorganic salts. The remaining crude mixture was purified by radial chromatography with 20:80 (ether/petroleum ether) to 40:60 (ether/petroleum ether) to give the protected catechol (158 mg, 83%). $^1$H NMR ($CDCl_3$): $\delta$ 7.01 (m, 3H), 6.83 (m, 4H), 5.26 (s, 4H), 5.22 (s, 4H), 3.68 (s, 6H), 3.52 (s, 6H), 3.05 (s, 6H), 1.47 (s, 18H). $^{13}$C NMR: $\delta$ 152.1, 150.9, 146.4, 144.2, 143.4, 137.9, 120.4, 115.5, 114.9, 111.0, 99.8, 96.4, 58.0, 56.9, 41.2, 35.9, 31.0. IR (film from $CH_2Cl_2$) $\nu$ ($cm^{-1}$): 2952.1, 1590.6, 1566.7, 1482.9, 1435.0, 1387.2, 1303.4, 1231.6, 1201.7, 1159.8, 1082.1, 1034.2, 1010.3, 956.4, 836.6. Anal. Calcd for $C_{36}H_{51}O_8N$: C, 69.09; H, 8.21; N, 2.23%. Found: C, 69.09; H, 8.25; N, 2.21%.

**Bis(catechol) 6.** To a 50 mL flask containing the protected bis(catechol) from the previous reaction (132 mg, 0.21 mmol) in 15 mL of methanol were added three drops of concentrated hydrochloric acid (12 M). The reaction mixture was refluxed for 12 h. Once cool, the solvent was removed under reduced pressure. Ether was added, and the solution was washed with a saturated solution of $NaHCO_3$ and then a saturated NaCl solution. The organic layer was dried with $Na_2SO_4$ and filtered, and the solvent was removed under reduced pressure to give **6** (95 mg, 100%). $^1$H NMR ($CDCl_3$): $\delta$ 7.08 (d, 2H, 1.29 Hz), 7.03 (s, 1H), 6.94 (d, 2H, 1.29 Hz), 6.91 (s, 2H), 5.73 (broad, 4H), 3.03 (s, 6H), 1.44 (s, 18H). $^{13}$C NMR: $\delta$ 152.0, 143.7, 143.6, 143.3, 137.3, 134.1, 119.1, 115.4, 112.7, 110.8, 41.4, 35.3, 30.0. IR (film from $CH_2Cl_2$) $\nu$ ($cm^{-1}$): 3506.8, 2954.5, 1584.1, 1484.2, 1448.9, 1407.8, 1366.7, 1302.0, 1249.1, 1196.3, 1143.4, 1084.6, 978.8, 943.6, 843.7, 796.7, 737.9. The bis(catechol) was used directly in the next step.

**5,5″-Di-*tert*-butyl-3,4,3″,4″-tetrakis-methoxymethoxy-5′-nitro-[1,1′,3′,1″]terphenyl.** A 100 mL flask containing 1,3-dibromo-5-nitrobenzene, **5**[42] (0.17 mL, 0.6 mmol), boronic acid **2**[40] (0.45 g, 1.51 mmol), $Na_2CO_3$ (2 M, 1.33 mL), and $Pd(PPh_3)_4$ (35 mg, 0.03 mmol) in toluene (20 mL) was pump-purged five times under nitrogen. The reaction mixture was refluxed for 54 h. Once cool, the solvent was removed under reduced pressure, ether was added, and the reaction mixture was filtered to remove inorganic solids. Following evaporation, the residue was subjected to radial chromatography, eluting with 5−15% ether/petroleum ether to give the protected bis(catechol) (300 mg, 79%). $^1$H NMR: $\delta$ 8.30 (s, 2H), 8.00 (s, 1H), 7.32 (s, 2H), 7.29 (s, 2H), 5.24 (s, 8H), 3.63 (s, 6H), 3.52 (s, 6H), 1.48 (s, 18H). $^{13}$C NMR: $\delta$ 150.6, 149.1, 146.7, 144.2, 143.4, 133.9, 131.8, 120.3, 119.8, 113.9, 99.2, 95.6, 57.7, 56.4, 35.5, 30.5. IR (film from $CH_2Cl_2$) $\nu$ ($cm^{-1}$): 2955.4, 1571.3, 1535.4, 1483.4, 1437.4, 1348.0, 1250.8, 1163.8, 1081.2, 1012.2, 957.3. Anal. Calcd for $C_{34}H_{45}O_{10}N$: C, 65.05; H, 7.22%. Found: C, 65.15; H, 7.20%.

**Bis(catechol) 8.** To a 50 mL flask containing the protected bis(catechol) (61 mg, 0.1 mmol) in 15 mL of methanol were added three drops of concentrated hydrochloric acid (12 M). The reaction mixture was refluxed for 12 h. Once cool, the solvent was removed under reduced pressure. Ether was added, and the solution was washed with a saturated solution of $NaHCO_3$ and then a saturated NaCl solution. The organic layer was dried with $Na_2SO_4$ and filtered, and the solvent was removed under reduced pressure to give **8** (44 mg, 100%). $^1$H NMR ($CDCl_3$): $\delta$ 8.25 (d, 2H, 1.56 Hz), 7.92 (t, 1H, 1.56 Hz), 7.14 (d, 2H, 2.04 Hz), 7.04 (d, 2H, 2.04 Hz), 5.84 (s, 2H), 5.40 (s, 2H), 1.48 (s, 18H). $^{13}$C NMR: $\delta$ 149.8, 144.8, 144.1, 144.0, 137.9, 131.6, 130.8, 120.0, 119.2, 112.6, 35.4, 29.9. IR (film from $CH_2Cl_2$) $\nu$ ($cm^{-1}$): 3506.8, 2954.5, 2860.5, 1595.8, 1525.3, 1501.8, 1443.1, 1419.6, 1337.3, 1307.9, 1255.0, 1190.4, 1149.3, 1084.6, 978.8, 961.2, 920.1, 855.4, 737.9. The bis(catechol) was used directly in the next step.

**Complex 1-NMe$_2$.** A flask containing **6** (39 mg, 87 $\mu$mol), $Tp^{Cum,Me}ZnOH$ (121 mg, 175 $\mu$mol), and 10 mL of 1:1 methanol/$CH_2Cl_2$ was stirred overnight open to air. The dark green precipitate was filtered off and dried in air and then vacuum to give the complex (26 mg, 80%). IR (film from $CH_2Cl_2$) $\nu$ ($cm^{-1}$): 2954.5, 2860.5, 2543.2, 1513.6, 1431.3, 1360.8, 1307.9, 1225.6, 1155.1, 1114.0, 1061.1, 978.8, 861.3, 837.8, 790.8. Anal. Calcd for $C_{106}H_{123}O_4N_{13}B_2Zn_2\cdot 0.5CH_2Cl_2$: C, 69.59; H, 6.79; N, 9.90%. Found: C, 69.68; H, 6.81; N, 10.02%. UV−Vis ($CH_2Cl_2$) $E_{max}$/$cm^{-1}$ (log $\epsilon$): 40 650 (4.74), 26 738 (4.39), 14 327 (3.37).

**Complex 1-*t*-Bu.** A flask containing **7** (130 mg, 281 $\mu$mol), $Tp^{Cum,Me}ZnOH$ (389 mg, 562 $\mu$mol), and 20 mL of 1:1 methanol/$CH_2Cl_2$ was stirred overnight open to air. The light green precipitate was filtered off and dried in air and then vacuum to give **1-*t*-Bu** (415 mg, 82%). IR (film from $CH_2Cl_2$) $\nu$ ($cm^{-1}$): 3060, 2957, 2925, 2868, 2536, 1574, 1548, 1520, 1467, 1440, 1365, 1178, 1061, 986, 837, 789. Anal. Calcd. for $C_{108}H_{126}B_2N_{12}O_4Zn_2$: C, 71.72; H, 6.96; N, 9.29%. Found: C, 71.35; H, 6.97; N, 9.34%. UV−Vis ($CH_2Cl_2$) $E_{max}$/$cm^{-1}$ (log $\epsilon$): 40 650 (5.13), 26 455 (4.36), 13 055 (3.08).

**Complex 1-NO$_2$.** A flask containing **8** (139 mg, 308 $\mu$mol), $Tp^{Cum,Me}ZnOH$ (426 mg, 616 $\mu$mol), and 20 mL of 1:1 methanol/$CH_2Cl_2$ was stirred overnight open to air. The olive green precipitate was filtered off and dried in air and then vacuum to give **1-NO$_2$** (450 mg, 81%). IR (film from $CH_2Cl_2$) $\nu$ ($cm^{-1}$): 2954.5, 2860.5, 2543.2, 1513.6, 1437.2, 1354.9, 1225.6, 1184.5, 1061.1, 978.8, 861.3, 831.9, 784.9. Anal. Calcd for $C_{104}H_{117}O_6N_{13}B_2Zn_2$: C, 69.49; H, 6.56; N, 10.12%. Found: C, 69.36; H, 6.50; N, 10.16%. UV−Vis ($CH_2Cl_2$) $E_{max}$/$cm^{-1}$ (log $\epsilon$): 40 984 (5.20), 26 882 (4.42), 12 594 (3.12).

**Crystallographic Structural Determinations.** The following experimental information was common for the structure determinations of **1-*t*-Bu** and **1-NO$_2$**. A suitable crystal was mounted on the end of a glass fiber and transferred to a standard Bruker SMART CCD-based X-ray diffractometer equipped with a graphite-monochromated normal focus Mo K$\alpha$ X-ray tube ($\lambda$ = 0.710 73 Å) and an LT-2 low-temperature device. The X-ray intensities were measured at 158(2) K. The tube was operated at 2 kW (50 kV, 40 mA). The frames were collected using a scan width of 0.3 in $\omega$ and $\phi$. All frames were integrated with the Bruker SAINT software package[61] using a narrow frame algorithm. The structures were solved and refined using Bruker SHELXTL version 5.10.[62] Analysis of the data showed negligible decay during data collection; the data were processed with SADABS[63] and corrected for absorption. All non-hydrogen atoms were refined anisotropically using a full matrix least squares based on $F^2$. Except for the Ni complex, hydrogen atom positions were derived from a difference Fourier map and were allowed to refine isotropically. Further specific experimental details are found in Table 1 and the Supporting Information.

**1-*t*-Bu.** The detector was placed at a distance 5.113 cm from the crystal. A total of 2332 frames were collected with an exposure time of 90 s/frame. The integration of the data yielded a total of 63 391 reflections to a maximum $2\theta$ value of 53.16° of which 21 029 were independent and 15 559 were greater than $2\sigma(I)$. The final cell constants

(57) Ruf, M.; Weis, K.; Vahrenkamp, H. *J. Chem. Soc., Chem. Commun.* **1994**, 135.
(58) Shultz, D. A.; Bodnar, S. H.; Vostrikova, K. E.; Kampf, J. W. *Inorg. Chem.* **2000**, *39*, 6091.
(59) Shultz, D. A.; Bodnar, S. H.; Kampf, J. W. *Chem. Commun.* **2001**, 93.
(60) Shultz, D. A.; Bodnar, S. H.; Kumar, R. K.; Lee, H.; Kampf, J. W. *Inorg. Chem.* **2001**, *40*, 546.
(61) *Saint Plus*, 6.02 ed.; Bruker Analytical X-ray: Madison, WI, 1999.
(62) Sheldrick, G. M. *SHELXTL*, 5.10 ed.; Bruker Analytical X-ray: Madison, WI, 1997.
(63) Sheldrick, G. M. *SADABS. Program for Empirical Absorption Correction of Area Detector Data*; University of Gottingen: Gottingen, Germany, 1996.

(Table 1) were based on the xyz centroids of 6223 reflections above $10\sigma(I)$. Full-matrix least-squares refinement based on $F^2$ converged at R1 = 0.0973 and wR2 = 0.2643 [based on $I > 2\sigma(I)$], R1 = 0.1257 and wR2 = 0.2880 for all data. The hydro-borate ligand bonded to Zn2 is disordered over two closely related orientations. Additional details are presented in Table 1 and the Supporting Information.

**1-$NO_2$.** The detector was placed at a distance 5.103 cm from the crystal. A total of 3779 frames were collected with an exposure time of 30 s/frame. The integration of the data yielded a total of 82 747 reflections to a maximum $2\theta$ value of 52.98° of which 21 107 were independent and 17 956 were greater than $2\sigma(I)$. The final cell constants (Table 1) were based on the *xyz* centroids of 7667 reflections above $10\sigma(I)$. Full-matrix least-squares refinement based on $F^2$ converged at R1 = 0.1231 and wR2 = 0.3197 [based on $I > 2\sigma(I)$], R1 = 0.1359 and wR2 = 0.3271 for all data. Additional details are presented in Table 1 and the Supporting Information.

**1-$NMe_2$.** A suitable crystal for data collection was selected and mounted with epoxy cement on the tip of a fine glass fiber. Data were collected at 173 K with a Siemens P4/CCD diffractometer with graphite-monochromated Mo Kα X-radiation ($\lambda$ = 0.710 73 Å). No symmetry higher than triclinic was observed in the diffraction and photographic data. *E*-Statistics suggested the centrosymmetric space group option $P\bar{1}$ that yielded chemically reasonable and computationally stable results of refinement. The structure was solved using direct methods, completed by subsequent difference Fourier syntheses, and refined by full-matrix least-squares procedures. The molecule cocrystallized with three molecules of dichloromethane in the asymmetric unit and six molecules in the unit cell. The high *R*-factor results from all samples examined diffracting weakly (average $I/\sigma$ = 6.6), which limited resolution, and our inability to fashion a reliable model for disorder seen in the solvent molecules. All non-hydrogen atoms were refined with anisotropic displacement coefficients, and all hydrogen atoms were treated as idealized contributions. All software and sources of the scattering factors are contained in the SHELXTL (5.1) program library.[62]

**Magnetochemistry.** Magnetic susceptibilities were measured on a Quantum Design MPMS-XL7 SQUID magnetometer using an applied field of 1 T for Curie plots. Saturation magnetization values (see Supporting Information) are consistent with the spin of the ground states as described in the text. Microcrystalline samples were loaded into the sample space of a Delrin sample holder and mounted to the sample rod using string. Data were corrected for sample holder and molecular diamagnetism using Pascal's constants and intermolecular interactions as described in the text.

**Acknowledgment.** This work was funded by the National Science Foundation (CHE-9910076). We thank the NSF for funds to help purchase the SQUID magnetometer (CHE-0091247).

**Supporting Information Available:** Crystallographic data, representative EPR Curie plot, saturation plots, and electronic absorption spectra (PDF). This material is available free of charge via the Internet at http://pubs.acs.org.

JA020154+